Cellulose (2019) 26:7253–7269
https://doi.org/10.1007/s10570-019-02618-3

ORIGINAL RESEARCH

Three-dimensional cellulose-hydroxyapatite nanocomposite enriched with dexamethasone loaded metal–organic framework: a local drug delivery system for bone tissue engineering

Chandrani Sarkar · Angshuman Ray Chowdhuri · Subhadra Garai · Jui Chakraborty · Sumanta Kumar Sahu

Received: 17 September 2018 / Accepted: 5 July 2019 / Published online: 9 July 2019

Abstract Three-dimensional cellulose-hydroxyapatite nanocomposite integrated with dexamethasone loaded metal organic framework (HA/DMOF) has been synthesized as a local drug delivery system for bone tissue engineering. Initially, in situ dexamethasone encapsulated metal–organic frameworks (DMOFs) were developed and characterized. The synthesized DMOFs are 60–80 nm in size with rhombohedral morphology. Results showed that nearly 16% dexamethasone (Dex) was loaded in DMOFs. These synthesized DMOF nanoparticles were efficiently integrated with carboxymethyl cellulose-hydroxyapatite nanocomposite for the development of three dimensional localized drug delivery system, namely, HA/DMOF. The synthesized HA/DMOF nanocomposite was structurally characterized using various techniques. The mechanical properties of HA/DMOFs were also measured by means of compression test. It was found that the compressive strength and compressive modulus of HA/DMOF nanocomposite are 16.3 ± 1.57 MPa and 0.54 ± 0.073 GPa respectively, which are in the range of cancellous bone. In-vitro release behaviour of Dex from both DMOFs and HA/DMOFs was examined in phosphate buffered solution. It was found that Dex molecules have been released very slowly from HA/DMOF nanocomposite compared to DMOF nanoparticles, and it was sustained for 4 weeks. Cytocompatibility of HA/DMOF nanocomposite was evaluated against pre-osteoblast MC3T3 cells. It was found that the synthesized HA/DMOF nanocomposite is compatible to MC3T3 cells. Moreover, the ALP activity and extracellular mineralization capability of cells were enhanced when cultured with HA/DMOF nanocomposite. Results showed that the synthesized HA/DMOF nanocomposite is a promising material for possible therapeutic as well as load-bearing orthopedic applications.

C. Sarkar · A. R. Chowdhuri · S. K. Sahu (✉)
Department of Applied Chemistry, Indian Institute of Technology (ISM), Dhanbad, Jharkhand 826004, India
e-mail: sksahu@iitism.ac.in; sumantchem@gmail.com

C. Sarkar · S. Garai
Advanced Material and Processes Division, CSIR-National Metallurgical Laboratory, Jamshedpur 831007, India

C. Sarkar
Department of Chemistry, Mahila College, Kolhan University, Chaibasa, Jharkhand 833201, India

A. R. Chowdhuri
Department of Chemistry, Indian Institute of Technology, Madras, Chennai 600036, India

J. Chakraborty
CSIR-Central Glass and Ceramic Research Institute, 196, Raja S.C. Mullick Road, Jadavpur, Kolkata 700 032, India

Graphic abstract

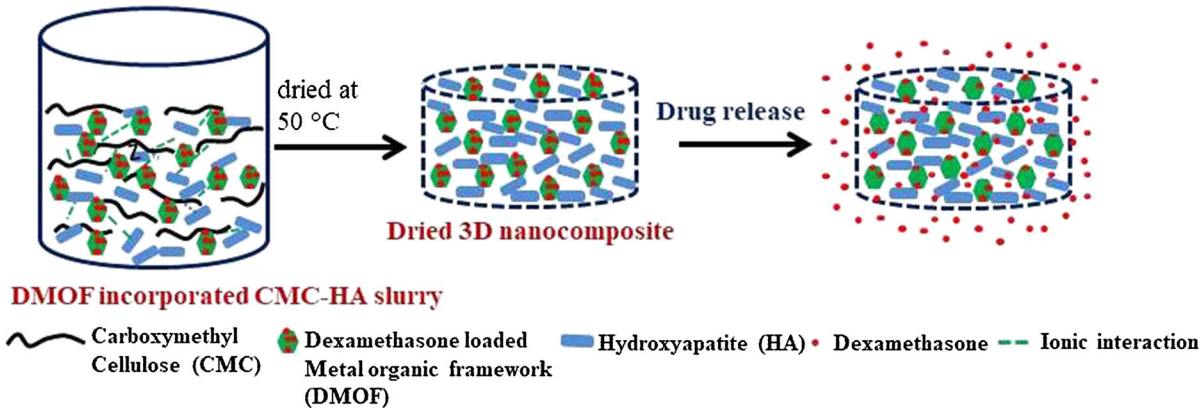

Keywords Hydroxyapatite · Carboxymethyl cellulose · Dexamethasone · Metal organic framework · Local drug delivery

Introduction

Nowadays, bone defect reconstruction is a prime concern in orthopedics due to wide range of population affected by bone related diseases and deformities. It increases the demand of advance material that can be used as bone substitutes. Biopolymer and its derived composites have been extensively used as biomaterials for the fabrication of medical devices due to their excellent biocompatibility, tunable chemical composition and good biological recognition (Wu et al. 2014). Cellulose is one of the most abundant, renewable biopolymer available worldwide. It is extensively used in cosmetic, pharmaceutical and food industries mainly as surfactants, stabilizers, thickener, emulsifier, binding agents and films. On increasing industrial demand, different types of cellulose derivatives were developed (Mondal 2019; Klemm et al. 2005). One of them is carboxymethyl cellulose (CMC), which one is Food and drug administration (FDA) approved hydrophilic and anionic derivative (Varma et al. 2014; Kumar et al. 2010). Moreover, it is usually added to formula for increasing the bioavailability of drug, and sometime used as filler with active ingredients in the tablet (Azzaoui et al. 2017; Qi et al. 2018). It is also used for treating dry eye after phacoemulsification, hemostatic material and also wound dressing as an adhesion-preventing material (Mondal 2019; Pei et al. 2015). Presently, it is used in tissue engineering field particularly for cartilage and skin regeneration (Varma et al. 2014; Basta et al. 2016).

On material point of view, CMC is considered as an excellent matrix material due to their extraordinary supramolecular structure, effective directionality and inherent rigidity (Garai and Sinha 2014; Rubler et al. 2011; Liuyun et al. 2009). Basically, cellulose-based composites are usually biocompatible, environmentally friendly, low cost, and also possess good mechanical properties. These composites are generally used for the manufacture of medical, electrochemical and bioenergy-storage devices (Nishio 2006; Cherian et al. 2011; Rubler et al. 2011; Adeosun et al. 2012; Guo et al. 2015; Gupta and Santhiya 2017; Narwade et al. 2017). In the biomedical field, cellulose-hydroxyapatite nanocomposites are extensively investigated (Hammonds et al. 2012; Garai and Sinha 2014; Azzaoui et al. 2015; Joshi et al. 2016; Park et al. 2017; Azzaoui et al. 2017). Because, hydroxyapatite is a calcium phosphate ceramic; which is chemically resembles with inorganic component of natural bone (Gouma et al. 2012). Nano-dimension of hydroxyapatite imparts good osteoconductivity and bone bonding ability to the composite (Gouma et al. 2012; Favi et al. 2016). However for better functioning, osteogenic compounds like growth factors and therapeutic molecules are combined with osteoconductive biomaterials and that combined system possesses properties analogous to autogenous bone (Martin and Bettencourt 2018). So, the current strategy in bone tissue

engineering is to design growth factors or therapeutic molecules loaded composite as local delivery system. Through this kind of system, the therapeutic molecules or growth factors directly release at the defect sites and induce osteogenesis (Mourino et al. 2013; Porter et al. 2009; Martin and Bettencourt 2018; Mourino and Boccaccini 2010). However, the cellulose-hydroxyapatite nanocomposite has been less studied in the drug delivery field. Till now, limited research groups have explored the applications of cellulose-hydroxyapatite nanocomposites in drug/growth factor delivery. Salama et al. (2016) synthesized carboxymethyl cellulose grafted poly(dimethylaminoethyl methacrylate)/hydroxyapatite composite for protein delivery. Recently, Fu et al. (2018) fabricated cellulose/hydroxyapatite nanocomposite by sonochemical method for protein/drug delivery. In those reports, it was noticed that cellulose-hydroxyapatite nanocomposites were synthesized in hydrogel (Salama et al. 2016) and sheet (Fu et al. 2018) forms/types for the delivery of protein/drug. Although, three dimensional nanocomposites can only be used as bone substitute/bone graft material. So, researchers have also synthesized three dimensional cellulose-hydroxyapatite nanocomposites for load bearing orthopedic applications (Garai and Sinha 2014; Joshi et al. 2016). However, the contribution of three dimensional cellulose-hydroxyapatite nanocomposite in drug delivery field has not been reported till now. Present study aimed to synthesize a three-dimensional cellulose-hydroxyapatite nanocomposite as local drug delivery system for therapeutic as well as load-bearing orthopedic applications.

Dexamethasone (Dex), a bioactive glucocorticoid steroid is a hydrophobic therapeutic molecule. This drug molecule has been widely studied in bone tissue engineering field, because it stimulates the up-regulation of bone-related genes such as alkaline phosphatase, osteocalcin, bone sialoprotein during osteogensis; and helps in differentiating stem cells to osteoblastic lineage (Xu et al. 2014; Silva et al. 2015; Qiu et al. 2016; Amjadian et al. 2016). However, Dex has very short biological half-life (< 4 h). Sometimes, it shows adverse effects on cells/tissues for long-time exposer with high concentration (Ali et al. 2013; Hur et al. 2016; Lim et al. 2016). For improving the bioavailability and maintenance of the Dex concentration during the treatment, researchers have incorporated Dex loaded carriers in hydroxyapatite composites for localized sustained delivery (Son et al. 2011; Zhou et al. 2015; Ghorbani et al. 2016; Gentile et al. 2016; Rumian et al. 2016; Leena et al. 2017; Zhang et al. 2018). Generally, polymeric microspheres and porous nanocarriers are used as drug delivery agent (Ali et al. 2013; Fratoddi et al. 2012; Bharti et al. 2015; Subhapradha et al. 2018). Though, the drug loading content and release is commonly depended on the nature of the carrier into which the drug is loaded. In this sense, porous materials are considered as a more advantageous drug carrier, because of having high specific surface area, and controllable pore size with well-ordered porous structure (Bharti et al. 2015). As an ultra-porous material, metal organic frameworks have drawn considerable attention in drug delivery due to their ultrahigh porosity (pore volume $\sim$ 1.04–4.40 cm^3g^{-1}), large surface areas (1000–7000 m^2g^{-1}), ease of formation and tunable functionality (Wuttke et al. 2017).

So, metal organic framework has been chosen as drug carrier in this study. Zeolitic imidazolate framework (ZIF-8) is a type of metal organic framework which is usually made up with zinc (Zn^{2+}) ion and imidazolate group (Chen et al. 2014). Here, Dex loaded ZIF-8 nanoparticles (DMOFs) were synthesized by a single step method and those synthesized DMOF nanoparticles have efficiently been integrated with cellulose-hydroxyapatite nanocomposite by a facile process. In-vitro release behavior of Dex from DMOFs and DMOFs integrated cellulose-hydroxyapatite nanocomposite (HA/DMOFs) was separately examined in phosphate buffered solution. It was found that Dex molecules have been released very slowly from HA/DMOF nanocomposite compared to DMOF nanoparticles. Furthermore, the mechanical properties of synthesized nanocomposite (HA/DMOF) are analogous to human cancellous bone. In in vitro cell study, it was observed that MC3T3 cells adhered well on the surface of HA/DMOF nanocomposite and proliferated with time. Moreover, MC3T3 cells showed high ALP activity and mineralization ability in presence of HA/DMOF nanocomposite. It shows that the synthesized HA/DMOF nanocomposite has great potential to be used as local drug delivery system for therapeutic as well as load-bearing orthopedic applications.

Materials and method

Materials used

Carboxymethyl cellulose as sodium salt (average M_w 250 kDa, degree of substitution 0.7), calcium nitrate tetrahydrate, zinc nitrate hexahydrate, diammonium hydrogen phosphate, methanol and ammonia were procured from Merck, India. 2-methyl imidazole was purchased from TCI chemicals. Fetal bovine serum (FBS), dimethyl sulpho-oxide (DMSO), phosphate buffered solution (PBS), α- minimum essential medium (α-MEM) and dexamethasone (Dex) were purchased from Himedia, India.

Synthesis of Dex loaded metal organic framework (DMOF)

Drug loaded nanoscale zeolite imidazolate framework (ZIF-8) has been prepared according to our previous reported method with slight modification (Chowdhuri et al. 2017). In brief, 150 mg zinc nitrate was added in 10 mL of methanol and stirred in magnetic stirrer. In the meantime, 300 mg 2-methylimidazole and 4 mg Dex were dissolved in another beaker containing 10 mL methanol. Then, Dex containing imidazole solution was dropwise added to zinc nitrate solution and stirred for 4 h. A milky white precipitate was obtained, that was collected by centrifugation and dried at 50 °C. The amount of Dex loaded in MOF nanoparticles was quantified by measuring the absorbance at 242 nm using UV–Vis spectrophotometer (Shimadzu 1800). Bare ZIF-8 nanoparticles were also prepared by the same procedure except the addition of Dex and labeled MOF.

Synthesis of three dimensional cellulose-hydroxyapatite nanocomposite supplemented with Dex loaded metal organic frameworks (HA/DMOFs)

Three-dimensional cellulose-hydroxyapatite nanocomposite enriched with Dex loaded metal organic frameworks was synthesized by following few simple steps. Initially, 0.5 g carboxymethyl cellulose was completely dissolved in 200 mL water. Afterwards, 50 mL aqueous calcium solution (0.99 M) was mixed with polymer solution. The pH of the mixed solution was maintained 10 by adding ammonia solution and aged overnight at normal temperature (25–30 °C). Next day, 100 mL aqueous phosphate solution (0.56 M) was mixed to the above solution and maintained pH 10. The whole mixture (slurry) was aged at normal room temperature for one week. After that, the slurry was washed with water. Meantime, 1.5 g DMOFs was ultrasonically dispersed in 80 mL water and added dropwise into washed slurry of cellulose-HA with continuous stirring. At the end, it was dried in an oven at 55 °C. Finally, three dimensional HA/DMOF nanocomposite was obtained. For comparative study, three-dimensional cellulose-hydroxyapatite nanocomposite was also prepared by following same procedure without the addition of DMOFs, and labelled HA. Millipore water has been used in each step.

Characterization

X-ray diffractions of synthesized nanoparticles and nanocomposites were collected using X-ray diffractometer [Phillips PW-1710]. Fourier transform infrared (FTIR) spectrometer [Agilent Carry 660 instrument] was used for recording the FTIR spectra of synthesized nanoparticles/nanocomposites. The surface morphology and microstructure of synthesized nanoparticles/nanocomposites were observed in scanning electron microscope (SEM) [Zeiss, Supra 55]. The particle size and the morphology of the synthesized nanoparticles/nanocomposites were characterized using Transmission electron microscopy (TEM) [JEM 2010 Electron Microscope JEOL] at 200 kV. The mechanical properties of synthesized nanocomposites ($\sim$ 8 mm $\times$ 4 mm $\times$ 4 mm) were evaluated using universal testing machine [Tinius Olsen (H25KS), ASTM D695]. In order to estimate the content of Dex in DMOF nanoparticles, thermogravimetric analysis of ZIF-8, Dex and DMOFs was carried out in Netzsch STA 449 C instrument at 10 °C min^{-1} heating rate in argon.

In-vitro drug loading and release study

To estimate the Dex loading content, DMOF nanoparticles were dissolved in 0.1 M aqueous solution of hydrochloric acid, and then the supernatant was analysed with a UV–Vis spectrophotometer (Shimadzu 1800). The weight of Dex in DMOF nanoparticles was determined using a standard curve method.

The Dex loading content (%) has been calculated by given equation

$$\text{DLC}\,(\%) = \frac{\text{Weight of drug in nanoparticles}}{\text{Weight of nanoparticles taken}} \times 100$$

The absorbance of acid treated MOF nanoparticles was also measured.

In the present study, we have investigated the in vitro release behavior of Dex from both DMOF nanoparticles and HA/DMOF nanocomposite. For DMOFs, 10 mg DMOFs were dispersed in 10 mL of PBS and incubated in shaking incubator at 37 °C for 2 weeks. Every day, 1 mL aliquot was withdrawn and replenished with 1 mL fresh PBS. For HA/DMOF, 10 mg HA/DMOF nanocomposite was immersed in a falcon containing 10 mL PBS and incubated at 37 °C. After that, aliquots were collected by following same procedure as in DMOFs, for maximum 4 weeks. The Dex release was quantified by measuring the absorbance of collected aliquots at 242 nm using UV–Vis spectrophotometer (Shimadzu 1800).

Cell culture

Preosteoblast MC3T3 cells were cultured in α-MEM media supplemented with 10% FBS and 1% penicillin/streptomycin in a humidified incubator at 37 °C with 5% CO_2. The media was replaced with fresh media in alternative days.

In-vitro cell viability test

The viability of MC3T3 cells were assessed by 3-[4, 5-dimethylthiazol-2-yl]-2,5-diphenyltetrazolium bromide (MTT) assay. In this assay, metabolically active cells transform the tetrazolium salt to deep purple colour formazan crystal. Thus, the absorbance of solubilized formazan is fairly proportional to live cells. In this study, 6×10^4 cells were cultured with HA and HA/DMOFs extracts for different time periods (1, 4 and 7 days). After incubation for desired period, MTT assay was performed by subsequently adding MTT solution [0.2 mg mL^{-1} in α-MEM] into well plate to develop formazan crystals. After that, crystals were solubilized by adding DMSO, and absorbance was measured at 595 nm.

In-vitro cell adhesion test

Initially, MC3T3 cells (6×10^4 cells) were seeded onto HA/DMOF nanocomposite (2 mm × 2 mm × 0.2 mm in size) and cultured for 1, 4 and 7 days respectively. At desired time, images of cells around HA/DMOF nanocomposite were captured using microscope (MOTIC AE31). Afterward, cell seeded samples were carefully rinsed with PBS, and cells were fixed with *p*-formaldehyde on the surface of HA/DMOF nanocomposite. Subsequently, cell fixed samples were carefully rinsed with PBS and dehydrated with graded ethanol. The morphology of attached cells on HA/DMOF nanocomposite was examined using scanning electron microscope (SEM).

ALP activity assay

The activity of alkaline phosphatase (ALP) enzyme is commonly measured for evaluating the osteogenic properties of biomaterial (Sarkar et al. 2018; Kuo et al. 2016). In this work, ALP activity of MC3T3 cells was quantified according the instruction given in ALP estimation kit [CCK035] of HiMedia. MC3T3 cells were cultured with synthesized nanocomposites (HA and HA/DMOF) for 2 weeks. After incubation for desired period, ALP assay was performed as per the instruction given in the Kit and the absorbance was measured at 405 nm. At final stage, ALP was normalized with total protein content. Total protein content was estimated by Bradford assay kit (HTBC005), HiMedia.

In-vitro extracellular mineralization study

In-vitro extracellular mineralization is generally evaluated by two extensively studied methods alizarin red (AR) staining and von kossa (VK) staining (Sarkar et al. 2018; Kuo et al. 2016). We have investigated the extracellular mineralization capability of MC3T3 cells in presence of HA and HA/DMOF nanocomposites by these methods. Initially, MC3T3 cells were cultured with HA and HA/DMOF for 1 week, 2 weeks and 3 weeks. After desired period of incubation, MC3T3 cells were fixed with *p*-formaldehyde and washed with biological water. For AR staining, 2 wt% alizarin solution was added and kept it at room temperature for half an hour. During this period, calcium ions of mineralized nodules were bound with dye and stained

with red color which was captured by MOTIC AE31 microscope. For VK staining, 1 wt% silver nitrate solution was added and kept under UV light for half an hour. Phosphate ions of mineralized nodules were bound with silver and developed deep brown color nodules which were captured by MOTIC AE31 microscope.

Statistical analysis

Statistical analyses of all quantitative assessments were executed by student's t test; the values are significant at $p < 0.05$. Data were presented as mean ± standard deviation (n = 3).

Result and discussion

This work demonstrates a simple route to synthesize three-dimensional cellulose-hydroxyapatite nanocomposite as local drug delivery system with the incorporation of drug loaded carriers. A schematic presentation of synthesis procedure is given in Fig. 1.

Characterization of as-synthesized MOFs and DMOFs

X-ray diffraction (XRD) was carried out to validate the formation of zeolitic imidazolate framework, ZIF-8. In the XRD patterns of MOFs and DMOFs (Fig. 2a), the characteristic diffractions correspond to the plane (011), (002), (112), (022), (013), (222), (114), (233), (134), (044), (235) of ZIF-8 are present at 2θ = 7.75°, 10.78°, 13.18°, 15.20°, 16.93°, 18.56°, 22.5°, 24.94°, 27.14°, 30.05°, 32.88° respectively (Chowdhuri et al. 2017; Ran et al. 2018). It indicates that the formation of ZIF-8 has not been hindered in presence of Dex molecules and, even, Dex loaded zeolitic imidazolate frameworks (DMOFs) were successfully formed. However, the characteristics peaks of Dex were not found in the XRD pattern of DMOFs that may be due to low content of Dex in ZIF-8 (Ran et al. 2018). It can also be assumed that Dex is present as an amorphous or disordered crystalline state inside the metal organic frameworks. Here, Dex has been encapsulated in the dissolved state or in form of molecular dispersion during the DMOF formation. So, the absence of the peaks distinctive to the Dex diffraction pattern suggested that it is in an amorphous state and molecularly dispersed in the metal organic frameworks (Ali et al. 2013). The encapsulation of Dex molecules in ZIF-8 was confirmed from UV–Vis spectra.

The formation of ZIF-8 was further confirmed from FTIR spectra (Fig. 2b). The FTIR spectra of as-synthesized MOFs shows broad band in the range of 3500–3400 cm^{-1}, assigned to N–H stretching of 2-methylimidazole of ZIF-8; whereas, two bands of C–H stretching (alkene and alkane) of imidazole unit are found at 3131 cm^{-1} and 2925 cm^{-1}, respectively. The C–N bands of ZIF-8 are found in the 1100–1400 cm^{-1} region. The band at 424 cm^{-1} is associated with Zn–N stretching of ZIF-8. From these characteristics bands, it can be confirmed that ZIF-8 is formed. In the FTIR spectrum of DMOFs, all the characteristics bands of ZIF-8 are found, and two new bands are observed at 1666 cm^{-1} and 890 cm^{-1} assigned to –C=O stretching and –C–H bending of Dex (Ran et al. 2018) respectively. Moreover, the N–H stretching band of ZIF-8 in DMOFs has been shifted to lower wavenumber at 3126 cm^{-1} that may be due to some physical interactions/hydrogen bonding between ZIF-8 and Dex. So, it has been concluded that Dex loaded metal organic frameworks were successfully formed by this one pot method.

The microstructure of as-synthesized MOFs and DMOFs are presented in Fig. 3. In the SEM image of MOFs (Fig. 3a), we can see that the nanoparticles are in rhombic dodecahedral morphology. This structure of MOF (ZIF-8) is due to the higher molar ratio of metal ions and ligands i.e. ½, that leads the formation of rhombic dodecahedron crystals (Parulkar and Brunelli 2017). In Fig. 3b, we can see that the morphology of DMOFs is almost same as in MOFs, did not found any major differences. Both nanoparticles are 60–80 nm in size. Similar type of morphology of MOFs and DMOFs was also observed in TEM images (Fig. 3c, d). The size of MOF and DMOF nanoparticles are 60 ± 10 nm and 60 ± 15 nm respectively. This shows that the presence of DEX molecule does not affect the formation and morphology of DMOFs (Ran et al. 2018).

The formation of Dex loaded zeolitic imidazolate frameworks i.e. DMOFs were confirmed from UV–Vis spectral analysis. In Fig. 4a, the pure Dex molecules exhibit an intense band at 242 nm whereas MOF nanoparticles did not show any band. However, DMOF nanoparticles give a band at the same region of

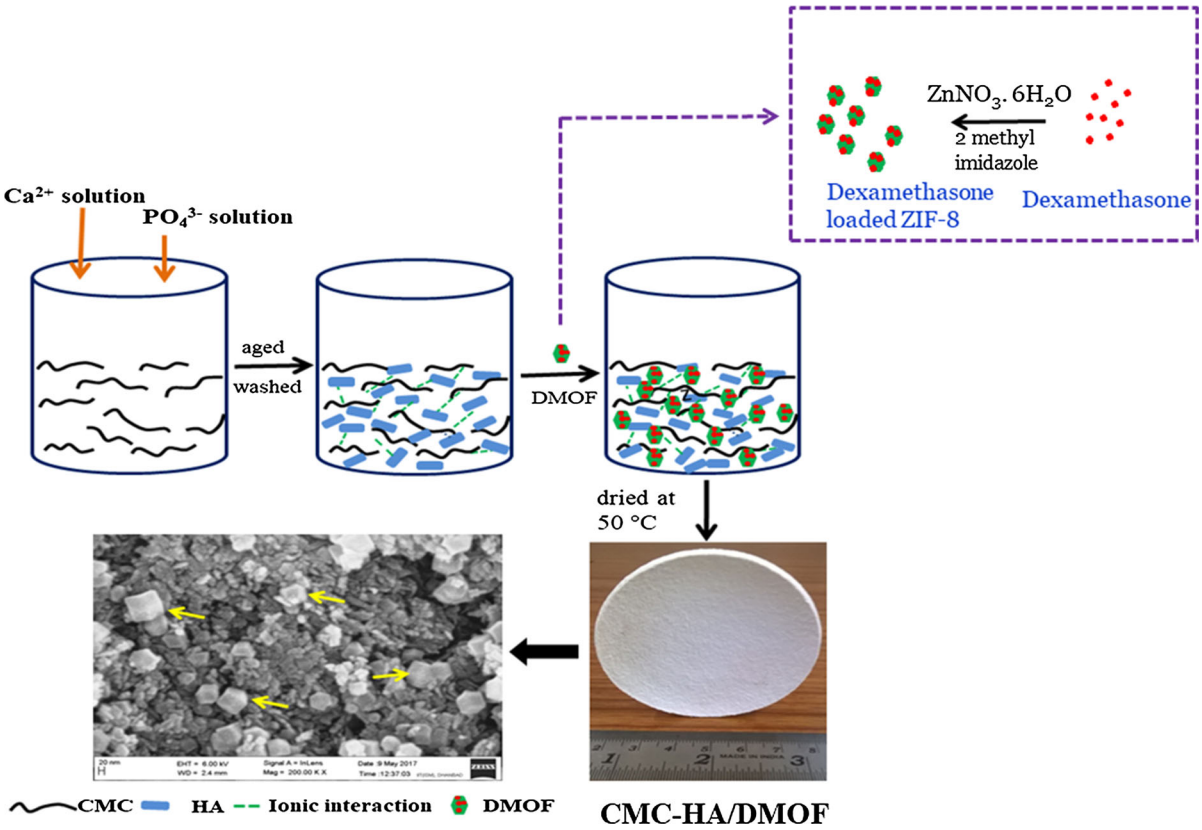

Fig. 1 The possible formation mechanism of three-dimensional cellulose-hydroxyapatite nanocomposite enriched with Dex loaded metal organic frameworks

Dex molecules i.e. 242 nm (Ran et al. 2018). It indicates that Dex molecules have been successfully encapsulated in ZIF-8 and showed a band at 242 nm. Furthermore, the Dex loading content in DMOFs was calculated, which is 16.6%.

The thermogravimetric (TG) curves of synthesized nanoparticles were presented in Fig. 4b. In case of MOFs, the major weight loss (36.1%) was occurred at 200–600 °C temperature range. This weight loss was attributed to the oxidation of organic imidazole part of ZIF-8 (He et al. 2014). The behaviour of TG curve in DMOFs is almost similar with MOFs. However, the weight loss of DMOFs is 42.6%, which is higher than MOFs that may be due to decomposition of encapsulated Dex molecule. Therefore, the content of encapsulated Dex in DMOFs was also determined from TG curve by following simple calculation:

$$\text{The weight loss (\%) of MOF i.e. ZIF-8 } \left[W_{loss(ZIF-8)}\right] = 36.1$$

$$\text{The weight loss (\%) of Dex } \left[W_{loss(Dex)}\right] = 76.2$$

Suppose, 100 g DMOF nanoparticles contained X g ZIF-8 and Y g Dex.

There existed two equations as follow

$$X + Y = 100$$

$$W_{loss(ZIF-8)} \times X + W_{loss(Dex)} \times Y = 42.6$$

X = 83.79% and Y = 16.21%

So, Dex content of the DMOF was 16.21%.

The Dex loading amount is nearly 16.2% which is in good agreement with UV–Vis result.

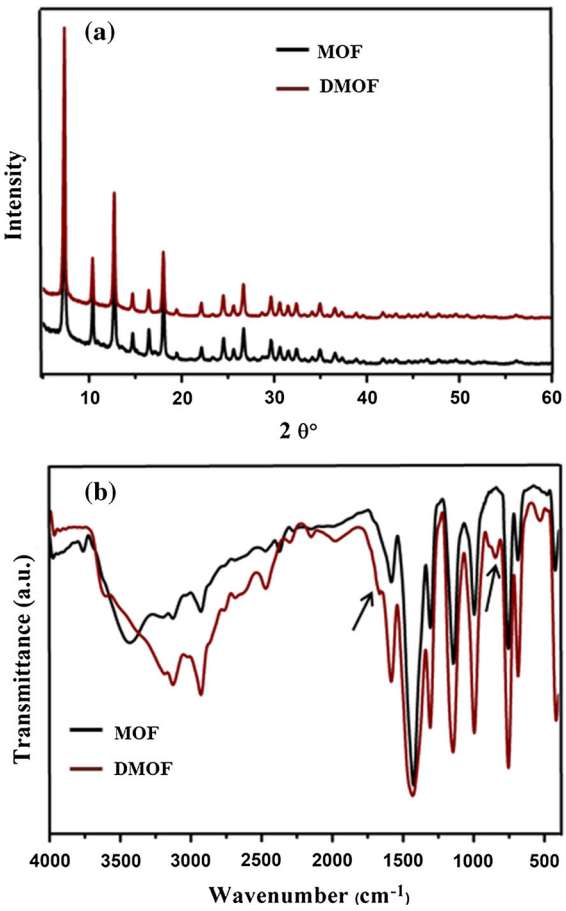

Fig. 2 **a** XRD patterns and **b** FTIR spectra of MOF and DMOF nanoparticles

Characterization of as-synthesized HA and HA/DMOF

The synthesized nanocomposites, HA and HA/DMOF were also systematically characterized by different techniques. The crystalline phases of synthesized nanocomposites were identified by XRD (Fig. 5a). In the XRD pattern of HA nanocomposite [in inset], the characteristic diffractions correspond to the (002), (102), (211), (202), (310), (222), (004), (213) and (511) reflections of hydroxyapatite (JCPDS file: 09-0432) are found at $2\theta = 26°$, 28°, 32°, 34°, 40°, 47°, 50°, 56°, 64° respectively (Zhang et al. 2018; Salama et al. 2016). In HA/DMOF, the characteristics peaks of both ZIF-8 and HA were found. It indicates the presence of both crystalline nanoparticles. As similar in Fig. 2a, no peak corresponds to Dex was observed in the XRD pattern of HA/DMOF.

The interactions among the different phases of nanocomposites were investigated by FTIR analysis (Fig. 5b). In the spectrum of HA nanocomposite, the strong bands at 1043 cm^{-1}, 608 cm^{-1} and 568 cm^{-1} attribute the vibrations of PO_4^{3-} group of hydroxyapatite. An overlapped band at 3428 cm^{-1} arises from the O–H stretching of hydroxyapatite and carboxymethyl cellulose. The bands at 1615 cm^{-1} and 1420 cm^{-1} assigned to asymmetric and symmetric COO^- stretching of carboxymethyl cellulose, respectively (Garai and Sinha 2014; Sarkar et al. 2018). These bands are also observed in the FTIR spectra of HA/DMOF nanocomposite. Additionally, strong characteristic bands of ZIF-8 at 2924 cm^{-1}, 1306 cm^{-1} and 420 cm^{-1} were also found; indicate the presence of ZIF-8. The representative band of Dex was found at 890 cm^{-1} in the spectrum of HA/DMOF nanocomposite. However, 1660 cm^{-1} band of Dex was not identifiable in HA/DMOF spectrum that may be due to the presence of other peaks at this region, and may also be due to low level of Dex compared to other components (Nadim et al. 2017). Noticeably, the OH band of HA/DMOFs was broaden and shifted to lower wavenumber that signify the interaction of hydroxyl groups of cellulose with Zn of ZIF-8 (Liang et al. 2017).

The surface morphology and microstructure of as-synthesized HA and HA/DMOF nanocomposites were observed by scanning electron microscope (SEM) and transmission electron microscope (TEM), which are given in Fig. 6. In SEM image (Fig. 6a) of HA nanocomposite, very small needle-like hydroxyapatite nanoparticles were observed, almost 40–60 nm in size. In HA/DMOF nanocomposite (Fig. 6b), similar needle-like morphology of hydroxyapatite was observed; in addition rhombic dodecahedral nanoparticles of DMOF (60–80 nm in size) were also found. In TEM image (Fig. 6c) of HA composite, we found agglomerates of those needle-like hydroxyapatite nanoparticles (almost 10 ± 3 nm in width and 40 ± 20 nm in length) due to cohesive interaction between CMC and hydroxyapatite nanoparticle. In Fig. 6d, we found DMOF nanoparticles in addition with hydroxyapatite nanoparticles, as similar observed in SEM image of HA/DMOF nanocomposites.

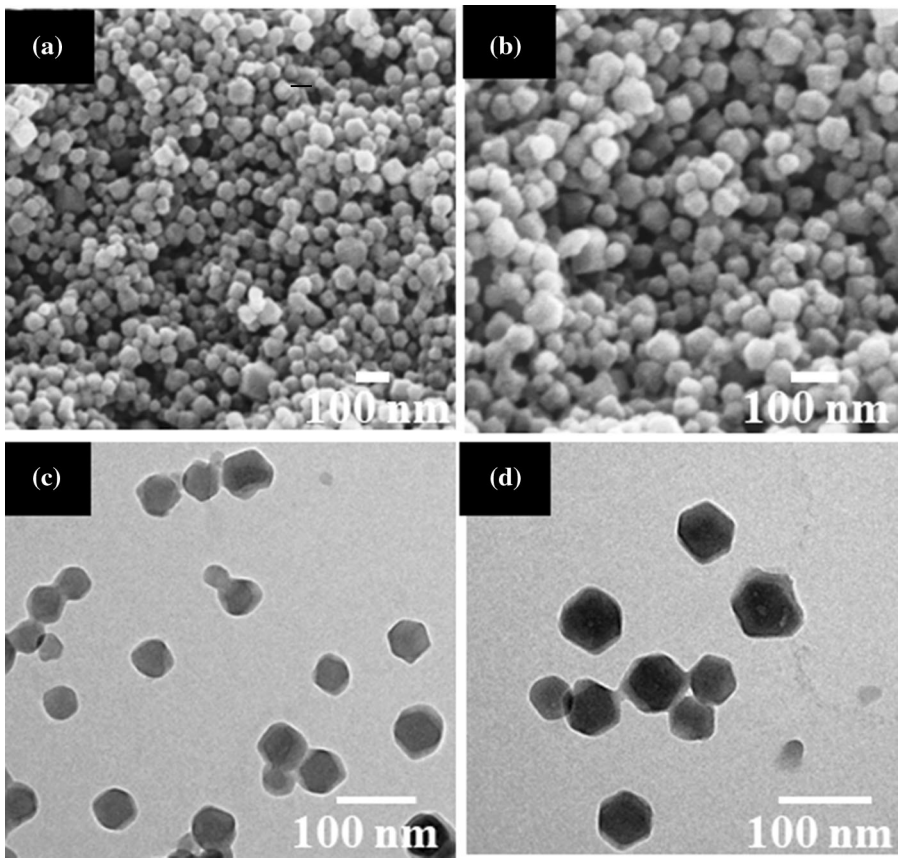

Fig. 3 SEM and TEM images of MOF (**a**, **c**) and DMOF (**b**, **d**) nanoparticles

Mechanical properties of HA and HA/DMOF nanocomposites

It is necessary to evaluate the mechanical properties of three-dimensional drug loaded composite for possible load-bearing orthopedic application. In this study, the mechanical properties of HA and HA/DMOF composites were evaluated by compression test. The stress–strain curves of HA and HA/DMOF are shown in Fig. 7. Both the composites visco-elastically deformed under compression; this type of deformation generally found in human bone (Fayyazbakhsh et al. 2017). It was also noticed that the compressive strength of HA (16.2 ± 1.83 MPa) and HA/DMOF (16.3 ± 1.57 MPa) nanocomposites are almost same; whereas the modulus of HA/DMOF composite (0.54 ± 0.073 GPa) is slightly higher than HA composite (0.36 ± 0.067 GPa). It attributes the interaction between ZIF-8 nanoparticles and cellulose, is one of the reasons for the enhancement of compressive modulus of HA/DMOF nanocomposite (Liang et al. 2017). However, the compressive strength and compressive modulus of both the composites are in the range of cancellous bone (Fayyazbakhsh et al. 2017).

In-vitro Dex release study

The release behaviour of Dex from DMOF nanoparticles and HA/DMOF nanocomposite were examined in PBS (pH-7.4) at 37 °C and presented in Fig. 8. The cumulative release of Dex from DMOFs was checked for 2 weeks (Fig. 8a). Nearly 28%, 60%, 77% and 89% Dex was released from DMOFs at day 1, day 3, day 7 and day 14 respectively. However, Dex was released from HA/DMOF nanocomposite in more controlled manner (Fig. 8b) and sustained for 4 weeks. About 8%, 16%, 35% and 60% Dex was released at day 1, day 3, day 7 and day 14 respectively.

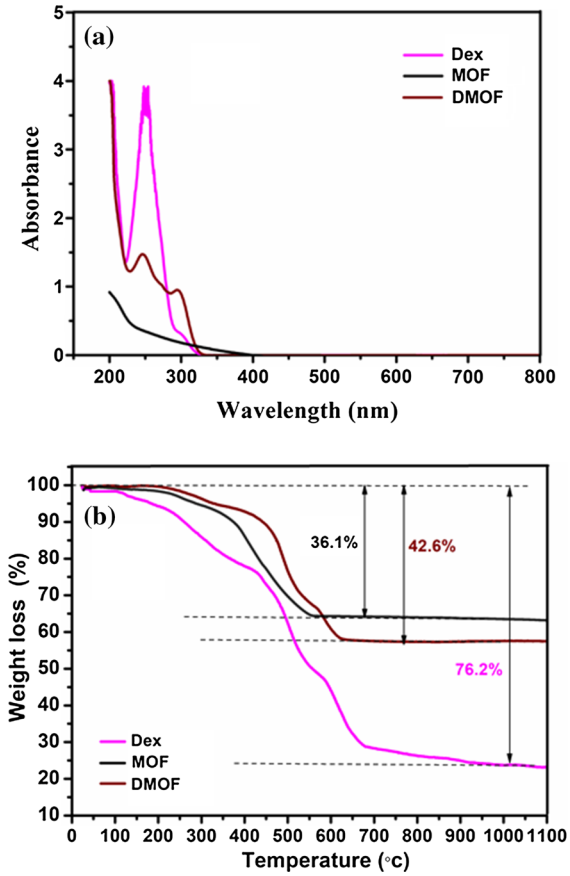

Fig. 4 **a** UV–Vis spectra **b** TG curves of Dex, MOF nanoparticles and DMOF nanoparticles

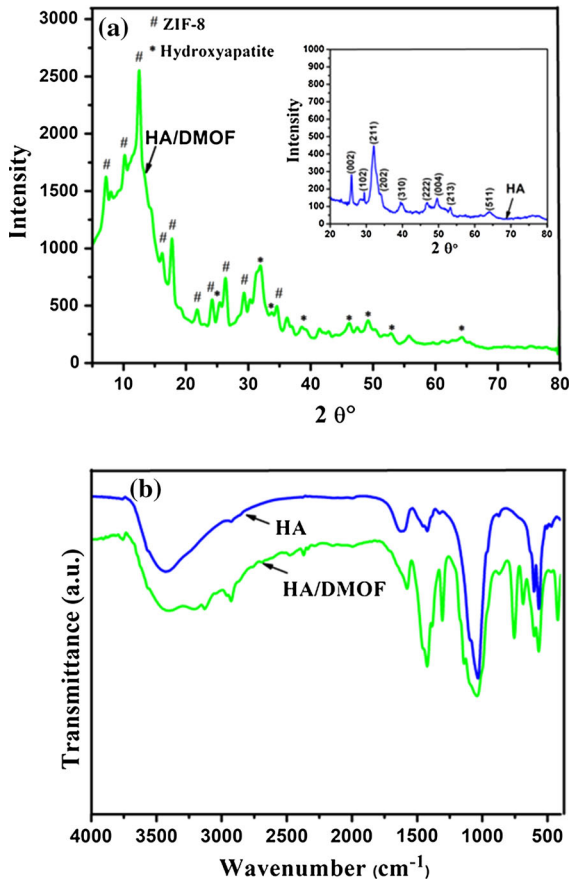

Fig. 5 **a** XRD patterns and **b** FTIR spectra of HA and HA/DMOF nanocomposites

Almost 75% Dex was released at day 28. It can be seen that less amount of Dex was released from HA/DMOF composite compared to DMOF at each time interval. Moreover, the behaviour of drug release curve of HA/DMOF nanocomposite is slightly different from DMOF nanoparticles (Fig. 8). DMOF curve exhibits slight burst release in the initial stage as a result of concentration gradient difference. After that a sustained release of Dex was observed up to day 14, whereas, the initial release of Dex from HA/DMOF nanocomposite was slow or more controlled. This is due to the less availability of DMOF nanoparticles in the surface part of HA/DMOF nanocomposite. After that, Dex was released from HA/DMOF nanocomposite at an intermediate rate, when the PBS reaches to the DMOF nanoparticles located at the inner core part of the HA/DMOF nanocomposite. Hence, the average diffusion path length of Dex molecule was increased in the case of HA/DMOF nanocomposite. Thus, HA/DMOF nanocomposite exhibited longer Dex release period than DMOF nanoparticles. It indicates that the Dex release from HA/DMOF nanocomposite was controlled by a combination of diffusion and transport mechanism (Son et al. 2011).

Compared with other reports, three dimensional Dex loaded nanocomposite (HA/DMOF) exhibits longer Dex release period and more controlled Dex release behaviour. In Son et al. report, 90% Dex was released from immobilized DEX-loaded PLGA microsphere on hydroxyapatite scaffold at day 28 (Son et al. 2011). Qiu et al. (2016) report, almost 75% Dex was released within 5 days from Dex loaded mesoporous silica nanoparticles incorporated poly lactic acid/poly caprolactone composite scaffold. In Yao et al. (2016) report, almost 73% Dex was released in PBS at day 6 with initial burst release. However, the behaviour of

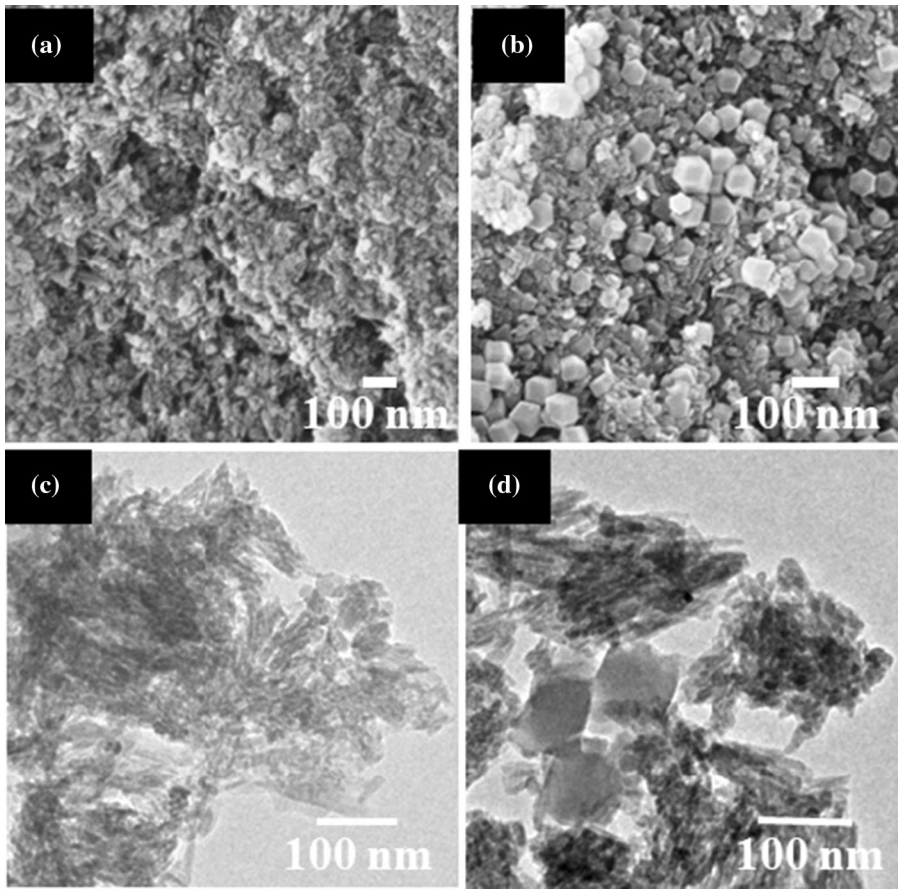

Fig. 6 SEM and TEM images of HA (**a**, **c**) and HA/DMOF (**b**, **d**) nanocomposites

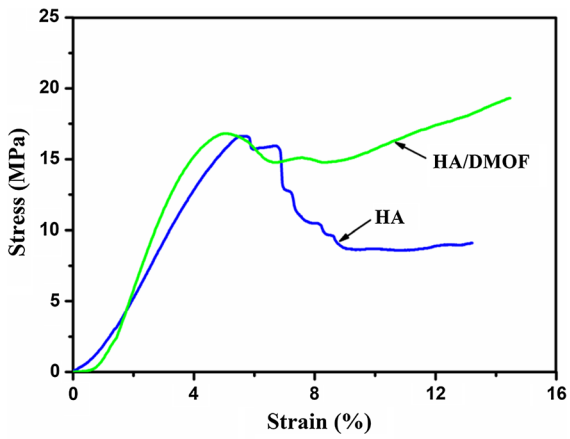

Fig. 7 Compressive stress versus strain curve of HA and HA/DMOF nanocomposites

Dex release curve of HA/DMOF is similar with the nature of dexamethasone loaded biphasic calcium phosphate nanoparticles/collagen composite in Chen et al. (2018) report, where almost 83% Dex was released at Day 35.

Cytocompatibility test

It is known that Dex has adverse effects on cells, when it is supplied at high doses for long periods of time (Espanol et al. 2016). The cytocompatibility of synthesized nanocomposites was quantitatively determined by MTT assay and represented in Fig. 9a. The test was carried out for different time periods i.e. 1, 4 and 7 days. It was observed that none of the composite shows any toxic effect, even the absorbance was

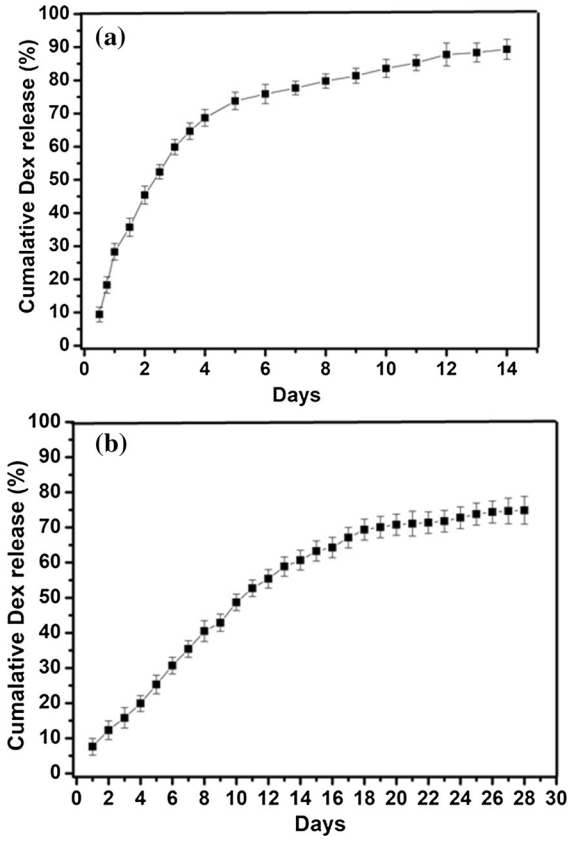

Fig. 8 In-vitro Dex release profile of **a** DMOFs and **b** HA/DMOFs

increased with culture time. It indicates that the cells are proliferated in presence of HA/DMOF nanocomposite, that can be further confirmed from Fig. 9b. In phase contrast images, we can see that the number of cells around the HA/DMOF composite was increased with culture time. We found the similar trend in SEM images where cell density on the surface of HA/DMOF nanocomposite was also increased with culture time. In addition, cells were appeared in fusiform and polygonal morphology with spicular-like pseudopodia indicated good cellular activity. From this observance, it was proved that Dex had no adverse effect on cell growth and cell attachment. Moreover, sustained release of Dex from HA/DMOF nanocomposite increased the activity of cells to proliferate (Son et al. 2011).

In-vitro cell differentiation study

In osteogensis, cell differentiation is a follow up phase after cell proliferation. Once the osteoblasts completely proliferate, they secrete collagen in the intercellular region and form collagenous matrix. Those extracellular collagenous matrices are mineralized by osteoblasts, hence, new bone tissue form (Silva et al. 2015). To investigate the osteogenic differentiation of MC3T3 cells in presence of HA and HA/DMOF nanocomposites, we have assessed the ALP activity of cells and in vitro mineralization by AR staining and VK staining. ALP is an enzyme secreted by cells during early matrix formation and maturation period (Kuo et al. 2016). Here, the ALP enzyme activity of cells was quantitatively measured and presented in Fig. 10a. It was found that the ALP activity of cells in presence of HA/DMOF nanocomposite is significantly higher than that of HA, both in first week and second week. This growing trend of ALP activity of cultured cells may be due to the combined effect of Dex and hydroxyapatite nanoparticles in HA/DMOF nanocomposite.

In-vitro extracellular mineralization was examined for 1 week, 2 weeks and 3 weeks by AR staining and VK staining (Fig. 10b). In HA/DMOF, red stained mineralized nodules (AR staining) of newly deposited calcium phosphate were found in first week. But, in HA composite, it was found in second week. The area of red stained mineralized nodule was increased with time in both the nanocomposites. However, in HA/DMOF, the color was more intense, indicating that the calcium phosphate was deposited more. This may be due to high ALP activity of cells in presence of HA/DMOF nanocomposite, promotes more mineralization. In VK staining, the phosphate groups of deposits are specifically stained with deep brown colour. The result of VK staining is reliable with AR staining shows dense brown mineralized nodules after 3 weeks cultured with HA/DMOF nanocomposite. These observations indicated that the sustained release of Dex from HA/DMOF system promotes cells for higher ALP activity and calcium deposition compared to HA composite. It may be due to synergetic effect of Dex and hydroxyapatite nanoparticles on the cell behavior that corresponds to more cell differentiation in presence of HA/DMOF nanocomposite (Amjadian et al. 2016).

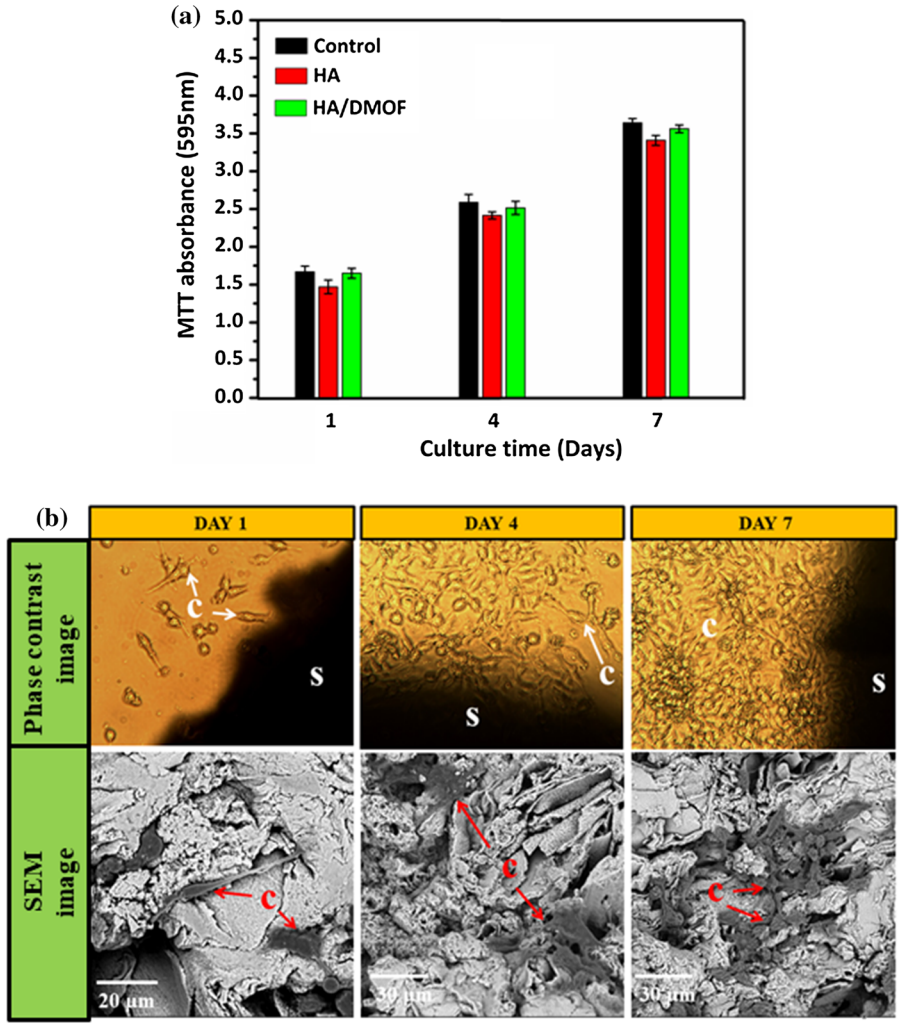

Fig. 9 **a** MTT assay; **b** phase contrast images and SEM images of MC3T3 cells cultured with HA/DMOF nanocomposite

Conclusion

The aim of this work was to synthesize three-dimensional cellulose-hydroxyapatite nanocomposite as local drug delivery system for therapeutic as well as load-bearing orthopedic applications. For this, in situ Dex encapsulated nanosized drug carrier, ZIF-8 has been synthesized by single step method. Those synthesized nanoparticles (DMOFs) were efficiently incorporated into cellulose-HA composite by simple mixing. In this way, three-dimensional cellulose-hydroxyapatite nanocomposite enriched with dexamethasone loaded metal–organic frameworks was successfully synthesized by a simple process. Moreover, it was found that the original shape and size of Dex encapsulated nanosized drug carrier were not disturbed after mixing; even the original shape i.e. rhombic dodecahedral of ZIF-8 was maintained in the composite. Drug release study showed that the Dex molecules were released in a sustained manner from synthesized nanocomposite throughout 4-week immersion period. In-vitro cell study showed that the synthesized nanocomposite is compatible to MC3T3 cells, and accelerates cells for proliferation and differentiation. Furthermore, the drug loaded cellulose-hydroxyapatite composite has compressive strength and modulus comparable to human cancellous bone. It shows the potential of Dex loaded cellulose-hydroxyapatite composite in localized drug delivery application particularly in load-bearing region. This study also opens up new scope in

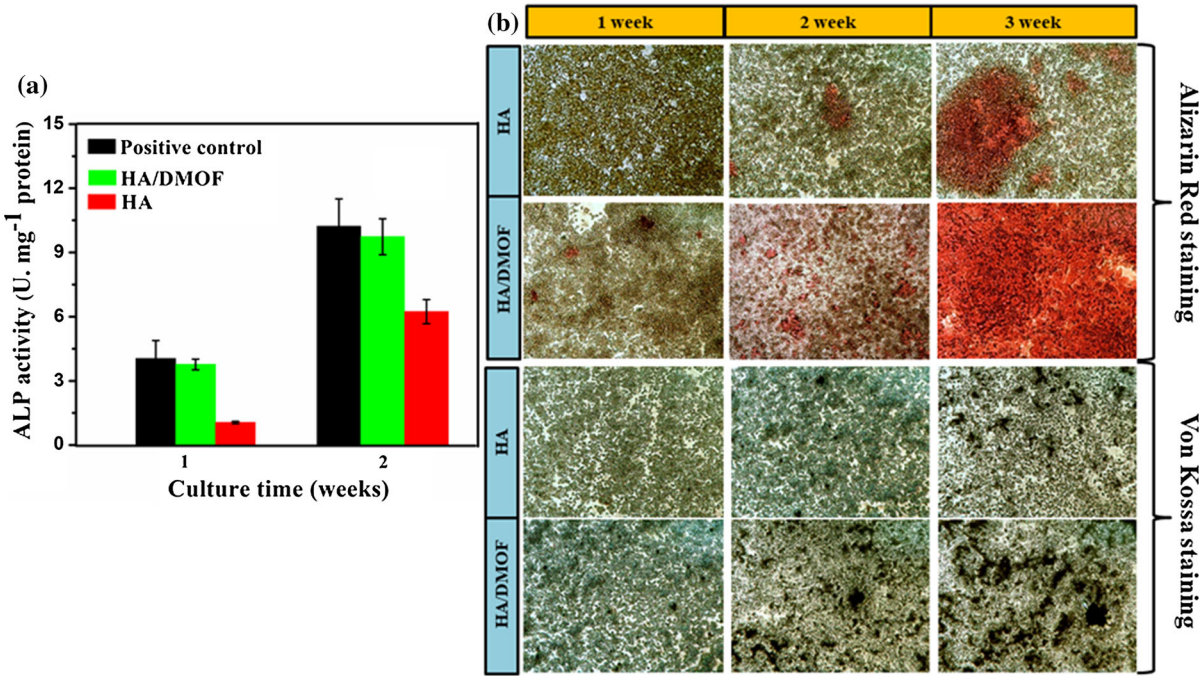

Fig. 10 **a** ALP assay **b** in-vitro extracellular mineralization of MC3T3 cells in presence of HA and HA/DMOF nanocomposites (Magnification = ×4)

therapeutic field for the delivery of other drugs or growth factors.

Acknowledgments The authors are grateful to the financial supports from project supporting group (OLP-0231) of CSIR-National Metallurgical Laboratory, India. The first author is also thankful to University Grant Commission for her fellowship. Funding was provided by University Grants Commission (Grant No. 061310230).

References

Adeosun SO, Lawal GI, Balogun SA, Akpan EI (2012) Review of green polymer nanocomposites. J Miner Mater Char Eng 11:385–416. https://doi.org/10.4236/jmmce.2012.114028

Ali H, Kalashnikova I, White MA, Sherman M, Rytting E (2013) Preparation, characterization and transport of dexamethasone-loaded polymeric nanoparticles across a human placental in vitro model. Int J Pharm 454:149–157. https://doi.org/10.1016/j.ijpharm.2013.07.010

Amjadian S, Seyedjafari E, Zeynali B, Shabani I (2016) The synergistic effect of nano-hydroxyapatite and dexamethasone in the fibrous delivery system of gelatin and poly(L-lactide) on the osteogenesis of mesenchymal stem cells. Int J Pharm 507:1–11. https://doi.org/10.1016/j.ijpharm.2016.04.032

Azzaoui K, Mejdoubi E, Lamhamdi A, Zaoui S, Berrabah M, Elidrissi A, Hammouti B, Fouda MMG, Deyab SSA (2015) Structure and properties of hydroxyapatite/Hydroxyethyl cellulose acetate composite films. Carbohydr Polym 115:170–176. https://doi.org/10.1016/j.carbpol.2014.08.089

Azzaoui K, Mejdoubi E, Lamhamdi A, Jodeh S, Hamed O, Berrabah M, Jerdioui S, Salghi R, Akartasse N, Errich A, Ríos Á, Zougagh M (2017) Preparation and characterization of biodegradable nanocomposites derived from carboxymethyl cellulose and hydroxyapatite. Carbohydr Polym 167:59–69. https://doi.org/10.1016/j.carbpol.2017.02.092

Basta AH, Saied HE, Deftar MME, Henawy AAE, Sheikh HHE, Shakour EHA, Hasanin MS (2016) Properties of modified carboxymethyl cellulose and its use as bioactive compound. Carbohydr Polym 153:641–651. https://doi.org/10.1016/j.carbpol.2016.07.051

Bharti C, Nagaich U, Pal AK, Gulati N (2015) Mesoporous silica nanoparticles in target drug delivery system: a review. Int J Pharm Investig 5:124–133. https://doi.org/10.4103/2230-973X.160844

Chen B, Yang Z, Zhu Y, Xia Y (2014) Zeolitic imidazolate framework materials: recent progress in synthesis and applications. J Mater Chem A 2:16811–16831. https://doi.org/10.1039/C4TA02984D

Chen Y, Kawazoe N, Chen G (2018) Preparation of dexamethasone-loaded biphasic calcium phosphate nanoparticles/collagen porous composite scaffolds for bone tissue engineering. Acta Biomater 67:341–353. https://doi.org/10.1016/j.actbio.2017.12.004

Cherian BM, Leao AL, de-Souza SF, Thomas S, Pothan LA, Kottaisamy M (2011) Cellulose nanocomposites for high-

performance applications. In: Kalia S, Kaith B, Kaur I (eds) Cellulose fibers: bio- and nano-polymer composites. Springer, Berlin, pp 539–587

Chowdhuri AR, Das B, Kumar A, Tripathy S, Roy S, Sahu SK (2017) One-pot synthesis of multifunctional nanoscale metal-organic frameworks as an effective antibacterial agent against multidrug-resistant *Staphylococcus aureus*. Nanotechnology 28:095102. https://doi.org/10.1088/1361-6528/aa57af

Espanol L, Larrea A, Andreu V, Mendoza G, Arruebo M, Sebastian V, Prado MSA, Hackmann ERMK, Santoro MIRM, Santamari J (2016) Dual encapsulation of hydrophobic and hydrophilic drugs in PLGA nanoparticles by a single-step method: drug delivery and cytotoxicity assays. RCS Adv 6:111060–111069. https://doi.org/10.1039/C6RA23620K

Favi PM, Ospina SP, Kachole M, Gao M, Atehortua L, Webster TJ (2016) Preparation and characterization of biodegradable nano hydroxyapatite–bacterial cellulose composites with well-defined honeycomb pore arrays for bone tissue engineering applications. Cellulose 23:1263–1282. https://doi.org/10.1007/s10570-016-0867-4

Fayyazbakhsh F, Hashjin MS, Keshtkar A, Shokrgozar MA, Dehghan MM, Larijani B (2017) Novel layered double hydroxides-hydroxyapatite/gelatin bone tissue engineering scaffolds: fabrication, characterization and in vivo study. Mater Sci Eng C 76:701–714. https://doi.org/10.1016/j.msec.2017.02.172

Fratoddi I, Venditti I, Cametti C, Palocci C, Chronopoulou L, Marino M, Acconcia F, Russo MV (2012) Functional polymeric nanoparticles for dexamethasone loading and release. Colloids Surf B 93:59–66. https://doi.org/10.1016/j.colsurfb.2011.12.008

Fu LH, Qi C, Liu YJ, Cao WT, Ma MG (2018) Sonochemical synthesis of cellulose/hydroxyapatite nanocomposites and their application in protein adsorption. Sci Rep 8:8292–8304. https://doi.org/10.1038/s41598-018-25566-7

Garai S, Sinha A (2014) Biomimetic nanocomposites of carboxymethyl cellulose-hydroxyapatite: novel three dimensional load bearing bone grafts. Colloids Surf B 115:182–190. https://doi.org/10.1016/j.colsurfb.2013.11.042

Gentile P, Nandagiri VK, Daly J, Chiono V, Mattu C, Turo CT, Ciardelli G, Ramtool Z (2016) Localised controlled release of simvastatin from porous chitosan–gelatin scaffolds engrafted with simvastatin loaded PLGA-microparticles for bone tissue engineering application. Mater Sci Eng C 59:249–257. https://doi.org/10.1016/j.msec.2015.10.014

Ghorbani F, Nojehdehianb H, Zamanian A (2016) Physicochemical and mechanical properties of freeze cast hydroxyapatite-gelatin scaffolds with dexamethasone loaded PLGA microspheres for hard tissue engineering applications. Mater Sci Eng C 69:208–220. https://doi.org/10.1016/j.msec.2016.06.079

Gouma P, Xue R, Goldbeck CP, Perrotta P, Balázsi C (2012) Nano-hydroxyapatite—cellulose acetate composites for growing of bone cells. Mater Sci Eng C 32:607–612. https://doi.org/10.1016/j.msec.2011.12.019

Guo X, Xue L, Lv W, Liu Q, Rumin Li, Li Z, Wang J (2015) Facile synthesis of magnetic carboxymethylcellulose nanocarriers for pH-responsive delivery of doxorubicin. New J Chem 39:7340–7347. https://doi.org/10.1039/C5NJ01190F

Gupta N, Santhiya D (2017) Role of cellulose functionality in bio-inspired synthesis of nano bioactive glass. Mater Sci Eng C 75:1206–1213. https://doi.org/10.1016/j.msec.2017.03.026

Hammonds RL, Harrison MS, Cravanas TC, Gazzola WH, Stephens CP, Benson RS (2012) Biomimetic hydroxyapatite powder from a bacterial cellulose scaffold. Cellulose 19:1923–1932. https://doi.org/10.1007/s10570-012-9767-4

He L, Li L, Zhang L, Xing S, Wang T, Li G, Wu X, Sua Z, Wang C (2014) ZIF-8 templated fabrication of rhombic dodecahedron-shaped ZnO@SiO2, ZIF-8@SiO2 yolk–shell and SiO2 hollow nanoparticles. CrystEngComm 16:6534–6537. https://doi.org/10.1039/C4CE00755G

Hur W, Park M, Lee JY, Kim MH, Lee SH, Park CG, Kim SN, Min HS, Min HJ, Chai JH, Lee SJ, Kim S, Choi TH, Choy YB (2016) Bioabsorbable bone plates enabled with local, sustained delivery of alendronate for bone regeneration. J Control Release 222:97–106. https://doi.org/10.1016/j.jconrel.2015.12.007

Joshi MK, Pant HR, Tiwari AP, Maharjan B, Liao N, Kim HJ, Park CH, Kim CS (2016) Three-dimensional cellulose sponge: fabrication, characterization, biomimetic mineralization, and in vitro cell infiltration. Carbohydr Polym 136:154–162. https://doi.org/10.1016/j.carbpol.2015.09.018

Klemm D, Heublein B, Fink HP, Bohn A (2005) Cellulose: fascinating biopolymer and sustainable raw material. Angew Chem Int Ed 44:3358–3393. https://doi.org/10.1002/anie.200460587

Kumar AP, Mohaideen KK, Alariqi SAS, Singh RP (2010) Preparation and characterization of bioceramic nanocomposites based on hydroxyapatite (HA) and carboxymethyl cellulose (CMC). Macromol Res 18:1160–1167. https://doi.org/10.1007/s13233-010-1208-3

Kuo ZK, Lai PL, Toh EKW, Weng CH, Tseng HW, Chang PZ, Chen CC, Cheng CM (2016) Osteogenic differentiation of preosteoblasts on a hemostatic gelatin sponge. Sci Rep 6:32884–32896. https://doi.org/10.1038/srep32884

Leena RS, Vairamani M, Selvamurugan N (2017) Alginate/gelatin scaffolds incorporated with Silibinin-loaded Chitosan nanoparticles for bone formation in vitro. Colloids Surf B 158:308–318. https://doi.org/10.1016/j.colsurfb.2017.06.048

Liang K, Wang R, Boutter M, Doherty CM, Mulet X, Richardson JJ (2017) Biomimetic mineralization of metal-organic frameworks around polysaccharides. Chem Commun 53:1249–1252. https://doi.org/10.1039/C6CC09680H

Lim HC, Nam OH, Kim M, Fiqi AE, Yun HM, Lee YM, Jin GZ, Lee HH, Kim HW, Kim EC (2016) Delivery of dexamethasone from bioactive nanofiber matrices stimulates odontogenesis of human dental pulp cells through integrin/BMP/mTOR signaling pathways. Int J Nanomed 11:2557–2567. https://doi.org/10.2147/IJN.S97846

Liuyun J, Yubao L, Chengdong X (2009) A novel composite membrane of chitosan-carboxymethyl cellulose polyelectrolyte complex membrane filled with nano-hydroxyapatite I. Preparation and properties. J Mater Sci Mater Med

20:1645–1652. https://doi.org/10.1007/s10856-009-3720-6
Martin V, Bettencourt A (2018) Bone regeneration: biomaterials as local delivery systems with improved osteoinductive properties. Mater Sci Eng C 82:363–371. https://doi.org/10.1016/j.msec.2017.04.038
Mondal MIH (2019) Cellulose-based superabsorbent hydrogels. Springer, Basel
Mourino V, Boccaccini AR (2010) Bone tissue engineering therapeutics: controlled drug delivery in three-dimensional scaffolds. J R Soc Interface 7:209–227. https://doi.org/10.1098/rsif.2009.0379
Mourino V, Cattalini JP, Roether JA, Dubey P, Roy I, Boccaccini AR (2013) Composite polymer-bioceramic scaffolds with drug delivery capability for bone tissue engineering. Expert Opin Drug Deliv 10:1353–1365. https://doi.org/10.1517/17425247.2013.808183
Nadim A, Khorasani SN, Kharaziha M, Davoodi SM (2017) Design and characterization of dexamethasone-loaded poly (glycerol sebacate)-poly caprolactone/gelatin scaffold by coaxial electro spinning for soft tissue engineering. Mater Sci Eng C 78:47–58. https://doi.org/10.1016/j.msec.2017.04.047
Narwade VN, Khairnar RS, Kokol V (2017) In-situ synthesised hydroxyapatite-loaded films based on cellulose nanofibrils for phenol removal from wastewater. Cellulose 24:4911–4925. https://doi.org/10.1007/s10570-017-1435-2
Nishio Y (2006) Material functionalization of cellulose and related polysaccharides via diverse microcompositions. In: Klemm D (ed) Polysaccharides II. Advances in polymer science. Springer, Berlin, pp 97–151
Park H, Kim MH, Yoon YI, Park WH (2017) One-pot synthesis of injectable methylcellulose hydrogel containing calcium phosphate nanoparticles. Carbohydr Polym 157:775–783. https://doi.org/10.1016/j.carbpol.2016.10.055
Parulkar A, Brunelli NA (2017) High-yield synthesis of ZIF-8 nanoparticles using stoichiometric reactants in a jet-mixing reactor. Ind Eng Chem Res 56:10384–10392. https://doi.org/10.1021/acs.iecr.7b02849
Pei Y, Ye D, Zhao Q, Wang X, Zhang C, Huang W, Zhang N, Liu S, Zhang L (2015) Effectively promoting wound healing with cellulose/gelatin sponges constructed directly from a cellulose solution. J Mater Chem B 3:7518–7528. https://doi.org/10.1039/C5TB00477B
Porter JR, Ruckh TT, Popat KC (2009) Bone tissue engineering: a review in bone biomimetics and drug delivery strategies. Biotechnol Prog 25:1539–1560. https://doi.org/10.1002/btpr.246
Qi P, Ohba S, Hara Y, Fuke M, Ogawa T, Ohta S, Ito T (2018) Fabrication of calcium phosphate-loaded carboxymethyl cellulose non-woven sheets for bone regeneration. Carbohydr Polym 189:322–330. https://doi.org/10.1016/j.carbpol.2018.02.050
Qiu K, Chen B, Nie W, Zhou X, Feng W, Wang W, Chen L, Mo X, Wei Y, He C (2016) Electrophoretic deposition of dexamethasone-loaded mesoporous silica nanoparticles onto poly(L–lactic acid)/poly(ε-caprolactone) composite scaffold for bone tissue engineering. ACS Appl Mater Interfaces 8:4137–4148. https://doi.org/10.1021/acsami.5b11879
Ran J, Zeng H, Cai J, Jiang P, Yan P, Zheng L, Bai Y, Shen X, Shi B, Tong H (2018) Rational design of a stable, effective, and sustained dexamethasone delivery platform on a titanium implant: an innovative application of metal organic frameworks in bone implants. Chem Eng J 333:20–33. https://doi.org/10.1016/j.cej.2017.09.145
Rubler A, Sakakibara K, Rosenau T (2011) Cellulose as matrix component of conducting films. Cellulose 18:937–944. https://doi.org/10.1007/s10570-011-9555-6
Rumian L, Tiainen H, Cibor U, Borkowicz MK, Wloch MB, Haugen HJ, Pamula E (2016) Ceramic scaffolds enriched with gentamicin loaded poly(lactide-co-glycolide) microparticles for prevention and treatment of bone tissue infections. Mater Sci Eng C 69:856–864. https://doi.org/10.1016/j.msec.2016.07.065
Salama A, Sakhawy ME, Kamel S (2016) Carboxymethyl cellulose based hybrid material for sustained release of protein drugs. Int J Biol Macromol 93:1647–1652. https://doi.org/10.1016/j.ijbiomac.2016.04.029
Sarkar C, Kumari P, Anuvrat K, Sahu SK, Chakraborty J, Garai S (2018) Synthesis and characterization of mechanically strong carboxymethyl cellulose–gelatin–hydroxyapatite nanocomposite for load-bearing orthopedic application. J Mater Sci 53:230–246. https://doi.org/10.1007/s10853-017-1528-1
Silva RF, Sasso GRS, Cerri ES, Simoes MJ, Cerri PS (2015) Biology of bone tissue: Structure, function, and factors that influence bone cells. BioMed Res Int. https://doi.org/10.1155/2015/421746
Son JS, Appleford M, Ong JL, Wenke JC, Kim JM, Choi SH, Oh DS (2011) Porous hydroxyapatite scaffold with three-dimensional localized drug delivery system using biodegradable microspheres. J Control Release 153:133–140. https://doi.org/10.1016/j.jconrel.2011.03.010
Subhapradha N, Abudhahir M, Aathira A, Srinivasan N, Moorthi A (2018) Polymer coated mesoporous ceramic for drug delivery in bone tissue engineering. Int J Biol Macromol 110:65–73. https://doi.org/10.1016/j.ijbiomac.2017.11.146
Varma DM, Gold GT, Taub PJ, Nicoll SB (2014) Injectable carboxymethylcellulose hydrogels for soft tissue filler applications. Acta Biomater 10:4996–5004. https://doi.org/10.1016/j.actbio.2014.08.013
Wu S, Liu X, Yeung KWK, Liu C, Yang X (2014) Biomimetic porous scaffolds for bone tissue engineering. Mater Sci Eng R 80:1–36. https://doi.org/10.1016/j.mser.2014.04.001
Wuttke S, Lismont M, Escudero A, Rungtaweevoranit B, Parak WJ (2017) Positioning metal-organic framework nanoparticles within the context of drug delivery—a comparison with mesoporous silica nanoparticles and dendrimers. Biomaterials 123:172–183. https://doi.org/10.1016/j.biomaterials.2017.01.025
Xu F, Yin M, Wu Y, Ding H, Song F, Wang J (2014) Effects of drying methods on the preparation of dexamethasone-loaded chitosan microspheres. Biomed Mater 9:055003. https://doi.org/10.1088/1748-6041/9/5/055003
Yao MZ, Huang-Fu MY, Liu HN, Wang XR, Sheng X, Gao JQ (2016) Fabrication and characterization of drug-loaded nano-hydroxyapatite/polyamide 66 scaffolds modified

with carbon nanotubes and silk fibroin. Int J Nanomed 11:6181–6194. https://doi.org/10.2147/IJN.S106929

Zhang B, Li H, He L, Han Z, Zhou T, Zhi W, Lu X, Lu X, Weng J (2018) Surface-decorated hydroxyapatite scaffold with on-demand delivery of dexamethasone and stromal cell derived factor-1 for enhanced osteogensis. Mater Sci Eng C 89:355–370. https://doi.org/10.1016/j.msec.2018.04.008

Zhou X, Feng W, Qiu K, Chen L, Wang W, Nie W, Mo X, He C (2015) BMP-2 derived peptide and dexamethasone incorporated mesoporous silica nanoparticles for enhanced osteogenic differentiation of bone mesenchymal stem cells. ACS Appl Mater Interfaces 7:15777–15789. https://doi.org/10.1021/acsami.5b02636